Acta Polytechnica **63**(2):89–102, 2023
https://doi.org/10.14311/AP.2023.63.0089
© 2023 The Author(s). Licensed under a CC-BY 4.0 licence
Published by the Czech Technical University in Prague

REMAPPING AND SIMULATION OF EFI SYSTEM FOR SI ENGINE USING PIGGYBACK ECU

Hau Than Diep[a], Gia Buu Nguyen[a], Barhm Mohamad[b,*]

[a] *Ho Chi Minh City University of Technology, Institute of International Education, Department of Automotive Engineering, HCMC, Vietnam*

[b] *Erbil Polytechnic University, Koya Technical Institute, Department of Petroleum Technology, 44001 Erbil, Iraq*

[*] corresponding author: pywand@gmail.com

Abstract. Electronic fuel injection (EFI) is a complex system comprising many parts, both mechanical and electronic, controlling an internal combustion engine. It carries out many different tasks. In motorsport, the most important thing to achieve is power optimisation. High power and engine responsiveness are often desired to gain a competitive edge. Usually, motorsport enthusiast will upgrade their stock vehicle with aftermarket components, such as higher rating turbo, longer duration camshafts, and exhaust system. These are difficult to carry out, time-consuming, and expensive tasks compared to the ECU calibration method. In Vietnam, most customers who want to change their vehicle's performance choose the Remap method on Factory ECU. By using the vehicle performance regulation method with a piggyback ECU, it is easier for the user to adjust the power than by the popular Remap method, the advantages being, for example, low cost and easy installation. Currently, there are very few documents describing and evaluating the effectiveness of a piggyback ECU installed in a vehicle. So, in this paper, an experimental reconstruction of an electronic fuel injection system with a piggyback ECU was performed, then the control algorithms of the electronic fuel injection system were simulated in LabVIEW, and the results were compared with the experiment, based on the simulation model of the control algorithm of the EFI system with many modes with different engine loads and speeds. The simulation results are used to evaluate the algorithm for the piggyback ECU.

Keywords: Internal combustion engine, engine control unit (ECU), engine management system (EMS), electronic fuel injection, engine control module (ECM).

1. Introduction

Over the last decades, the automotive industry has been increasingly incorporating new engine technologies [1], with major innovations in the Electrical/Electronic (E/E) systems [2]. Due to the complexity of new developments, the most important parameters, such as highest power, lowest emissions, and best fuel economy, heavily depend on the AFR values, an example being shown in Figure 1 [3]. Modern control systems of internal combustion engines with spark ignition are very complex units [4–7]. The Engine Management System (EMS) consists of the Engine Control Module (ECM) as well as various electrical/electronic components, such as sensors, actuators, and relays. It monitors the real-time operating conditions of the engine and issues control commands to multiple actuators, such as injectors, spark plugs, and a throttle valve [8]. Increasing the engine's performance involves increasing the engine outputs, power and torque, and decreasing the engine input, specific fuel consumption [9]. The engine outputs depend on many operating parameters, such as air-fuel ratio, compression ratio, intake air temperature and pressure, engine load and speed, ignition timing (for a spark ignition engine), injection parameter, and swirling design (for a compression ignition engine [10].

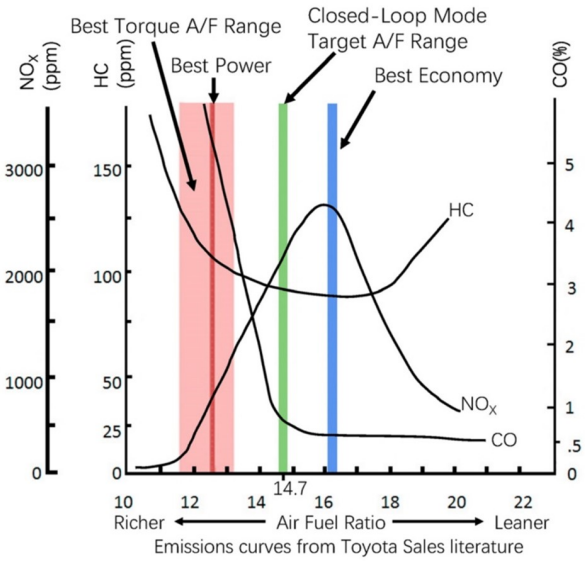

Figure 1. Engine performance and emissions based on the air-fuel ratio for gasoline. Source: Initial-training-free online sequential extreme learning machine-based adaptive engine air-fuel ratio control.

To optimise and enhance the abovementioned parameters, one can use a piggyback ECU, without

Item	Specification
Engine displacement (V_d)	2494 cc (2.5 l)
Crankshaft revolutions per power stroke (Cps)	2
Ideal gas constant for air and burned gas mixture (R_{air})	286.9
Engine speed (N)	800–6500 RPM
Stroke	4-stroke
Cylinder configuration	In-line 6 cylinders
Forced induction	Naturally aspirated

Table 1. Engine specifications.

modifying the factory ECU, so no basic or default features would get lost. The cost of this solution is fairly low as compared to more complex modifications [11], which is why so many owners tune their cars with a piggyback ECU. A Piggyback program generally costs a third or quarter of the original ECU or a standalone ECU price. We are also working on a method for measuring the overall car performance during on-road experiments [12–14]. The main objective of this research is to develop and present a concept of improving the general vehicle performance, measuring the actual impact during an on-road real-time experiment, and to describe our conceptual framework for a future implementation [15]. There are many algorithms developed for engine control in the automotive industry, but the documentation is rarely disclosed to public. Therefore, this paper will focus on simulating the operation algorithm of an electronic fuel injection system. The rest of the paper is organised as follows; first, the paper presents the theoretical basics of an algorithm calculation method; second, the simulation results are shown; third, the experimental and simulation results are compared and analysed, and finally, the article ends with conclusions.

2. Theoretical Basis

2.1. The vehicle used in the experiment

BMW E39 2003 is used as the experimental vehicle in this research. It has the 2.5L BMW M54B25 engine, naturally aspirated, with six cylinders.

Table 1 shows the engine specifications, which are used to calculate volumetric efficiency. To calculate the volumetric efficiency, several parameters, such as engine displacement, crankshaft revolutions per power stroke, and ideal gas constant for air and burned gas mixture, are needed.

2.2. Engine volumetric efficiency

To calculate the mass airflow (MAF) in a spark-ignition (SI) engine, one can configure the spark ignition and engine block to use speed-density mass airflow (MAF). The speed-density model uses the speed-density equation to control the engine air mass flow rate. The equation relates the engine MAF to the manifold gas pressure (MAP), engine speed, and intake manifold gas temperature. Consider using this air

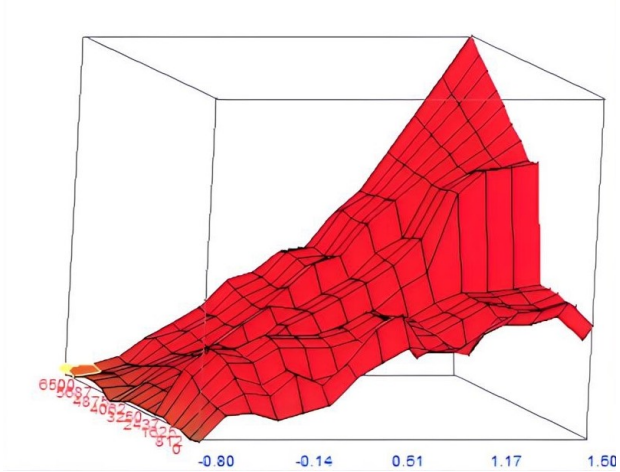

Figure 2. Volumetric efficiency lookup table.

mass flow model in simple convention engine designs where variable valve train technology is not in use [16]. To determine the air mass flow, the speed–density air mass flow model applies this momentum–density equations to the manifold gas pressure and gas temperature [16].

$$\dot{m}_{intk} = \frac{MAPV_d\, N \left[\frac{1\,\mathrm{min}}{60\,\mathrm{s}}\right]}{Cps\, R_{air}\, MAT} n_v\,, \tag{1}$$

$$\dot{m}_{air} = y_{intk,air}\, \dot{m}_{intk}\,. \tag{2}$$

The speed-density mass airflow (MAF) model uses a VE (volumetric efficiency) lookup table to correct the ideal MAF.

The VE lookup table (shown in Figure 2), f_{n_v}, is a function of the engine speed and intake manifold absolute pressure.

$$n_v = f_{n_v}(MAP, N)\,, \tag{3}$$

where:

n_v is the engine volumetric efficiency, dimensionless,

MAP is the intake manifold absolute pressure, in kPa,

N is the engine speed, in RPM.

To develop the volumetric efficiency table, we use the measured intake manifold gas pressure (MAP), air

mass flow rate (MAF), engine speed, and intake manifold gas temperature (IAT) from engine performance testing [16].

$$n_v = \frac{Cps\, R_{air}\, MAT}{MAPV_d\, N\left[\frac{1\,\mathrm{min}}{60\,\mathrm{s}}\right]}\dot{m}_{air}\,. \tag{4}$$

2.3. Fuel injection pulse width

The fuel injection system flowchart (shown in Figure 3) shows how the DET3 Piggyback ECU operates to compute the necessary fuel dose for the engine at different load and RPM conditions. The ECU reads LOAD values to determine the amount of air entering the engine and the load is calculated from the internal MAP sensor of the DET3 device. The ECU also reads RPM values to determine the speed of the engine, which is calculated from the Crankshaft position sensor. However, the ECU needs some signals, such as ECT and TPS, to enrich the fuel dose. At the same time, the fuel pump unit still works independently, not based on DET3, it is controlled by MS43.

The fuel injection pulse width is calculated using mass of air by the following equation:

$$\Delta T = \frac{p_{air}\cdot V_d\cdot N\cdot n_v}{R\cdot T_{air}\cdot AFR\cdot Inj.flowcoeff.\cdot 2}\,, \tag{5}$$

where:

ΔT is the basic fuel injection pulse width,

AFR is the ratio of air to fuel,

$Inj.flowcoeff.$ is the correction factor.

The final pulse width is composed of a basic fuel pulse width along with different correction factors and is calculated by using:

$$\Delta T_f = \Delta T\cdot f_{gf}\cdot f_{st}\cdot f_{as}\cdot f_{wp}\cdot f_{cl}\cdot f_{bv}\,, \tag{6}$$

where:

ΔT_f is the final pulse width,

f_{gf} is the global fuel enrichment factor,

f_{st} is the start correction factor,

f_{as} is the after-start correction factor,

f_{wp} is the warm-up correction factor,

f_{cl} is the closed-loop correction factor,

f_{bv} is the battery voltage correction factor.

2.4. Ignition Timing

Factors affecting the Ignition timing:

(1.) The speed of the engine,

(2.) The burning rate of the mixture:

- The density of the charge in the mixture,
- Homogeneity of the mixture,
- Quality, Air-Fuel ratio of the mixture,

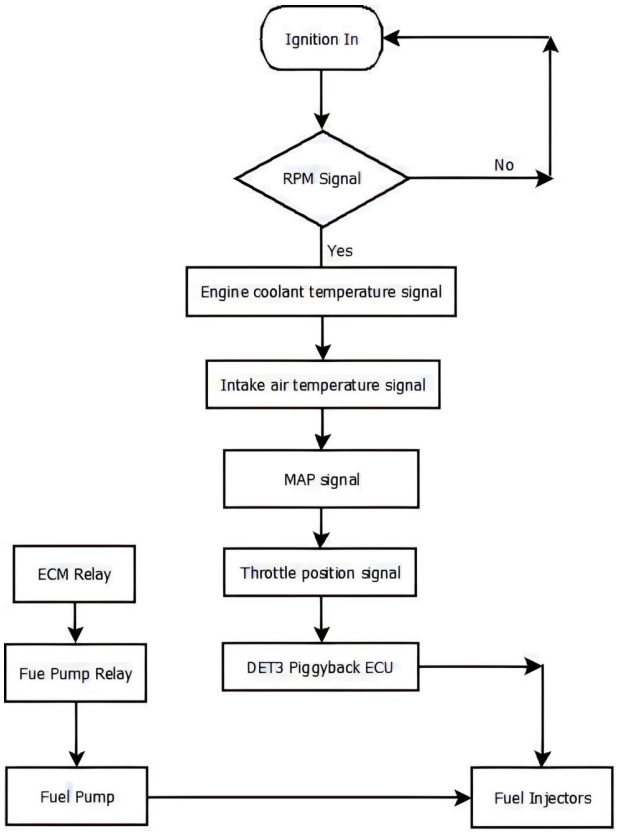

Figure 3. Fuel injection system flowchart.

- The number of residual gases present,

(3.) Load condition [17].

There are two basic factors to determine the ignition angle position in the ignition timing table:

- Engine load,
- Engine cycle position.

2.5. Ignition advance and retard

Ignition advance is the number of degrees before the top-dead-centre (BTDC) at which the spark occurs.

The ignition angle is modified at:

(1.) Ignition Advance when the speed increases,

(2.) Ignition retard when the load increases.

As the engine speed increases, the ignition advanced angle needs to increase since the air/fuel mixture combustion time is almost unchanged. If the ignition advance angle remains unchanged, the point of combustion pressure peak will move forward, resulting in a loss of power. If the point of the combustion pressure peak is too early and before the TDC, the pressure wave will slow down the speed of the piston travelling upwards and may cause a detonation (knock) that can cause damage to the engine. If the point of combustion pressure peak is too late, the pressure wave will 'pursue' the piston travelling downwards during the combustion stroke and most of the energy will be lost. Therefore, the ignition advance needs to be increased

to bring the point of combustion peak just after the TDC [18].

The optimal level of advancing the ignition varies by the engine and fuel used, hence the timing map of different fuel-using engines will vary. The ignition advance can be used as an addition to control emissions. Large ignition advances will promote the formation of O_2 in the exhaust gases and increase engine power (to an extent), but will also decrease the engine's fuel consumption [18].

The amount of time taken for a fuel/air mixture to combust depends mainly on the richness of the fuel mixture. When an engine is under a low load, the air/fuel mixture is lean, so it will need a higher ignition advance for a slow combustion. When the engine is under load, a richer air/fuel mixture is used to deliver more power. This rich mixture has a much faster combustion time, so the degree of ignition advance needs to be reduced to keep the combustion pressure peak well after the TDC. Load mapping is used to achieve this variation of ignition advance in modern engines. Information is sent from either a throttle potentiometer or a manifold pressure sensor indicating how much the engine is under load. Therefore, the load mapping will change the ignition advance based on the engine's speed and load [18].

2.6. Piggyback ECU Ecumaster DET3

The device (shown in Figure 4) is used for the current experiment with a naturally aspirated engine and the results are compared with the basic fuel injection pulse width algorithm. This ECU uses the "Fuel Implant" technology, which can directly control the injector opening time by using two algorithms: Speed Density algorithm and Alpha-N algorithm. They can control the fuel dose independently and do not depend on the factory ECU.

The overall wiring diagram is shown in Figure 5, with sensors, such as Crankshaft position sensor (CKP), throttle position sensor (TPS), engine coolant temperature sensor (CLT), and intake air temperature (IAT), being wired by tap method. The wideband oxygen sensor and injector outputs were wired directly to the DET3. The manifold absolute pressure was measured directly at the intake manifold by the sensor built in DET3.

The DET3 device is located in the engine compartment (shown in Figure 6), in the same place as the Siemens MS43 ECU. The colour of the wires is displayed in Figure 6. The red wire at pin 1 on DET3 is the power supply after the ignition switch, which uses 12 V. The brown wire at pin 9 on DET3 is the ignition signal used to read the RPM. The black wire at pin 11 on DET3 is the DET3's ground. The yellow wire at pin 13 on DET3 is the TPS signal. The orange wire at pin 15 on DET3 is the engine coolant temperature sensor. The green wire at pin 16 on DET3 is the intake air temperature sensor. The purple and blue wires at pins 18 and 20, respectively, are power

Figure 4. Piggyback ECU Ecumaster DET3. Source: Ecumaster.

output wires used for injectors, which are divided in pairs. Finally, the black wire at pin 19 is also used for feeding the power outputs.

The factory ECU may turn into a limp mode when the injectors are connected to the DET3 because of the lack of load on the outputs controlling the injectors. To solve this problem, we simulate the load of the injectors with the help of resistors. First, we need to calculate the right resistance value by using this equation:

$$P = U * U/R\,, \tag{7}$$

where:

P – the calculated resistor's power,

U – the power voltage (usually 13.5 V),

R – the injector's resistance.

Since the injector has a resistance of 14 Ω, the resistor's power equals to 13 W. So, in this case, it is enough to use the 15 W resistor. Because resistors give off a significant amount of heat, they were placed in "safe" regions (shown in Figure 7).

The coolant temperature sensor is calibrated by using a 10 kΩ resistor. In the original ECU, there is a resistor (Rx), which, together with the temperature sensor, creates the voltage divider. To configure the temperature sensor, a resistor Rx value and the characteristics of the resistance of the temperature sensor should be provided.

To calculate the resistance of the resistor Rx in the ECU, we should:

Disconnect the connector from the temperature sensor,

Check the voltage while the ignition is on and save it as Uin.

Then, connect the resistor of the known resistance in the sensor's plug (e.g. 10 K) Rk (in Ω). Then, measure the voltage again and save it as U_{out}. Rx is calculated by this equation:

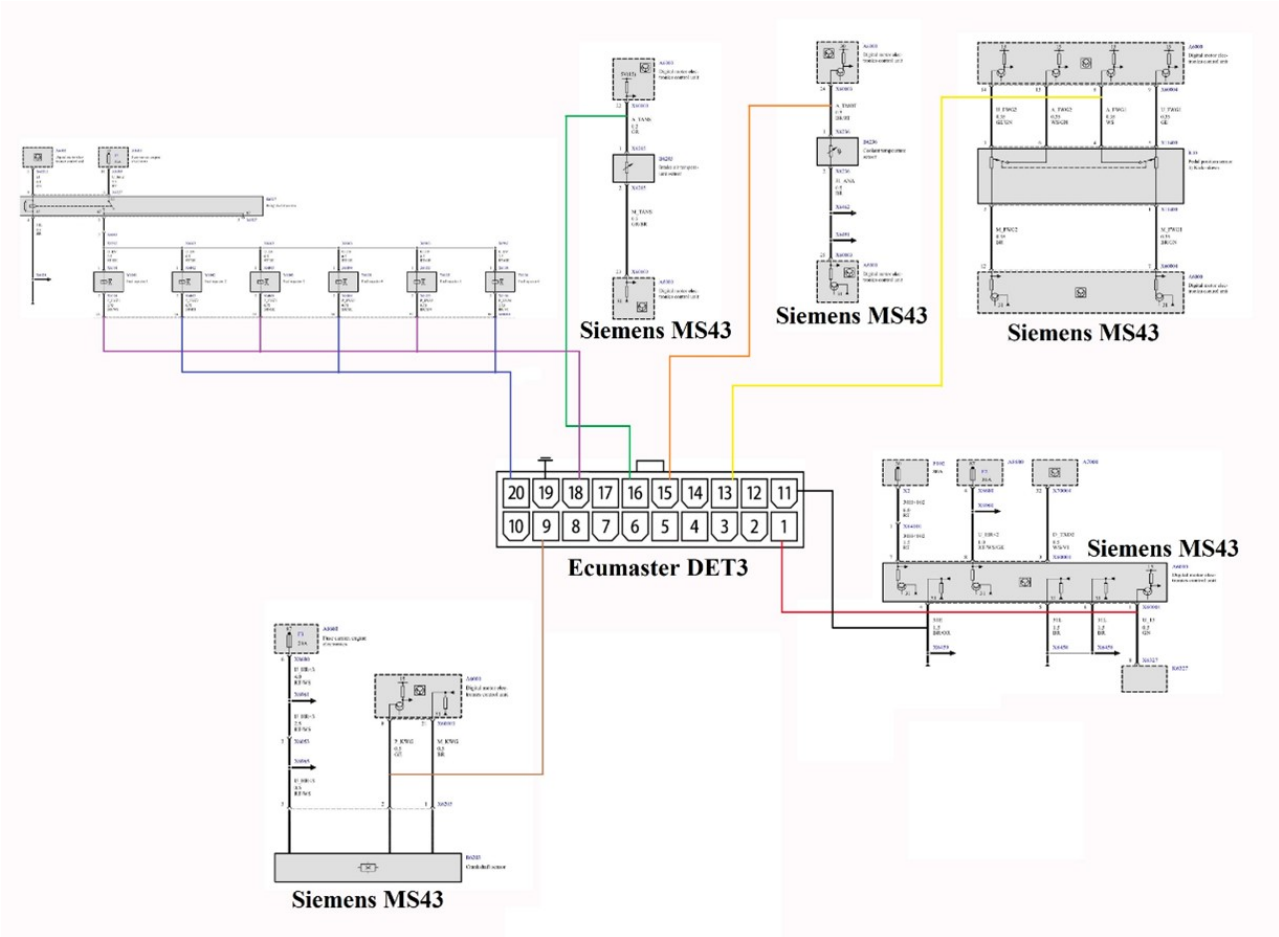

FIGURE 5. Overall wiring diagram of DET3 and Siemens MS43.

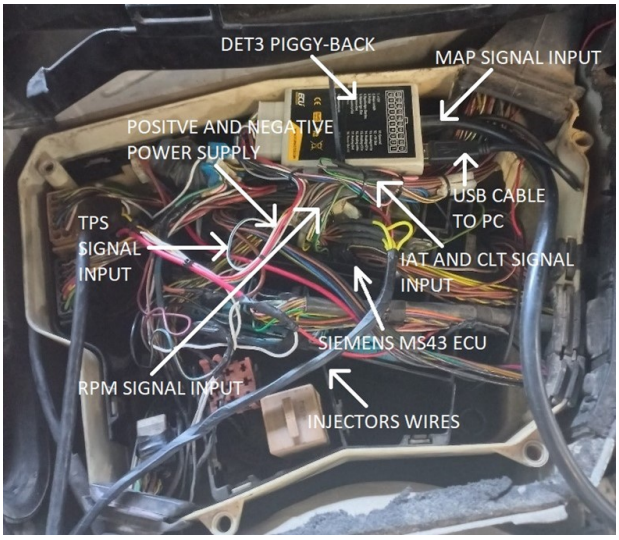

FIGURE 6. DET3 was placed in the engine compartment of the vehicle.

$$Rx = Rk * (U_{in} - U_{out})/U_{out}\,. \tag{8}$$

$$Rx = 9,780 * (4.96 - 4.58)/4.58 = 811\,\Omega\,.$$

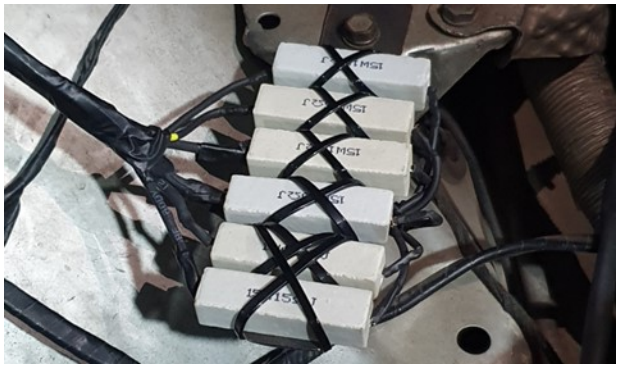

FIGURE 7. 15 W resistors for injectors used for preventing factory ECU turning into limp mode.

As we have the Rx value, we move to the firmware DET3 Fuel Implant to calibrate the sensors, where we set the previously calculated Rx resistor value of 811 Ω. The black line on the graph shows the characteristics of the sensor's resistance, the red line shows the voltage characteristics of the voltage divider (shown in Figure 8).

The rules for connecting and calibrating the air temperature sensor (IAT) are the same as those for the coolant temperature sensor so we just need to calculate the Rx value. Figure 9 shows the calibration

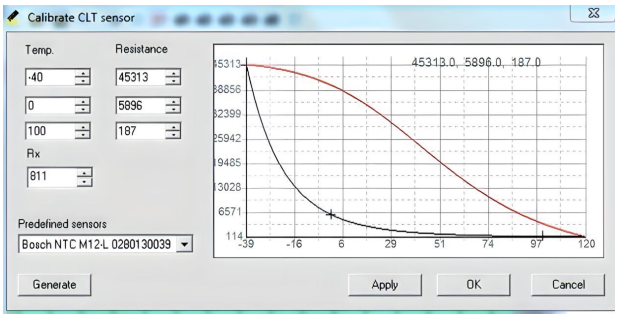

Figure 8. Calibration task of CLT sensor in the firmware.

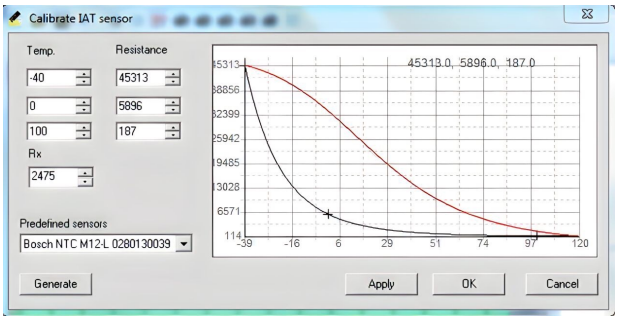

Figure 9. Calibration task of IAT sensor in the firmware.

of the IAT sensor.

$$Rx = 9,780 * (5 - 3.99)/3.99 = 2475\,\Omega\,.$$

3. Tuning and Simulation

3.1. Tuning Piggyback ECU

The VE table area is 16×16 (shown in Figure 10), which is also the main table. The main table often uses a common set of axes. The most common is the engine RPM and the load (in kPa) of the manifold pressure or fill percentage. The combination of engine speed and engine load tells the ECU a lot about what the engine is being asked to do. To make tuning easier, the base map has to be divided into "zones" and observe what's happening in each of those regions. It is divided into 7 zones, which will be present (shown in Figure 10). With zone 1, 2, 3, and 4 corresponding to the Idle and Cruise region, the AFR value in these regions has to be around 14.7 to achieve fuel economy. In zone 5, the engine is at a high speed and medium load, the engine has to be cooled, and the AFR value should be at around 13.5. Zone 6 is the WOT region, the AFR value has to be between 12.41 and 11.77 for the best performance. Zone 7 is the deceleration region, the software automatically cuts off the fuel.

3.2. Fuel injection pulse width simulation

The simulation model was made by LabVIEW software to simulate the controlling of the fuel injection pulse width based on the speed-density algorithm. The Front Panel (shown in Figure 11) was coded in G language through Block Diagram (shown in Figure 12) to control the fuel injection pulse width depending on input parameters (signals).

Inputs signals are the following:

- Engine rotation speed;
- Manifold absolute pressure;
- Intake air temperature;
- Volumetric efficiency;

The operation of the block diagram (shown in Figure 12) is based on how we adjust the engine load (MAP) and the engine speed (RPM) will give the corresponding value on the VE table. From the VE table, the MAP, air density in percentage, and INJCONST values can be used to calculate the corresponding fuel injection pulse width value.

3.3. Ignition timing simulation

The simulation model was made by LabVIEW software to simulate the controlling of the ignition timing. The Front Panel (shown in Figure 13) was coded in G language through Block Diagram (shown in Figure 14) to control the ignition timing based on the ignition timing table (shown in Figure 15), depending on engine speed and MAP.

By changing the values of engine load and engine speed, we can determine the ignition angle from the ignition timing table (shown in Figure 15). Based on that, when keeping the engine speed value unchanged and increasing the engine load values, the waveform of the ignition angle shows that the ignition timing will be retarded when the engine load increases (shown in Figure 16). Conversely, when keeping the engine load value unchanged and increasing the engine speed values, the waveform of ignition angle shows that the ignition timing will be advanced when the engine speed increases (shown in Figure 17).

The operation of the block diagram (shown in Figure 14) is based on adjusting the engine load (MAP), and consequently the engine speed (RPM) giving the corresponding value on the ignition timing table. From there, it will give the output of ignition angles for different engine loads and engine speeds in a waveform chart.

4. Results and Discussions

4.1. Experiment Testing

Racebox device (shown in Figure 18) was used to measure the performance stats of our vehicle before and after remapping the EFI system. It measures 0–100 km·h^{-1} acceleration with over 99.5 % measurement accuracy to a hundred of a second, compared to official lap/drag timing equipment.

The experiment testing before and after remapping the EFI system is carried out on the same road with the same conditions, and the same weight. The parameters and Fuel Map are tracked directly onboard

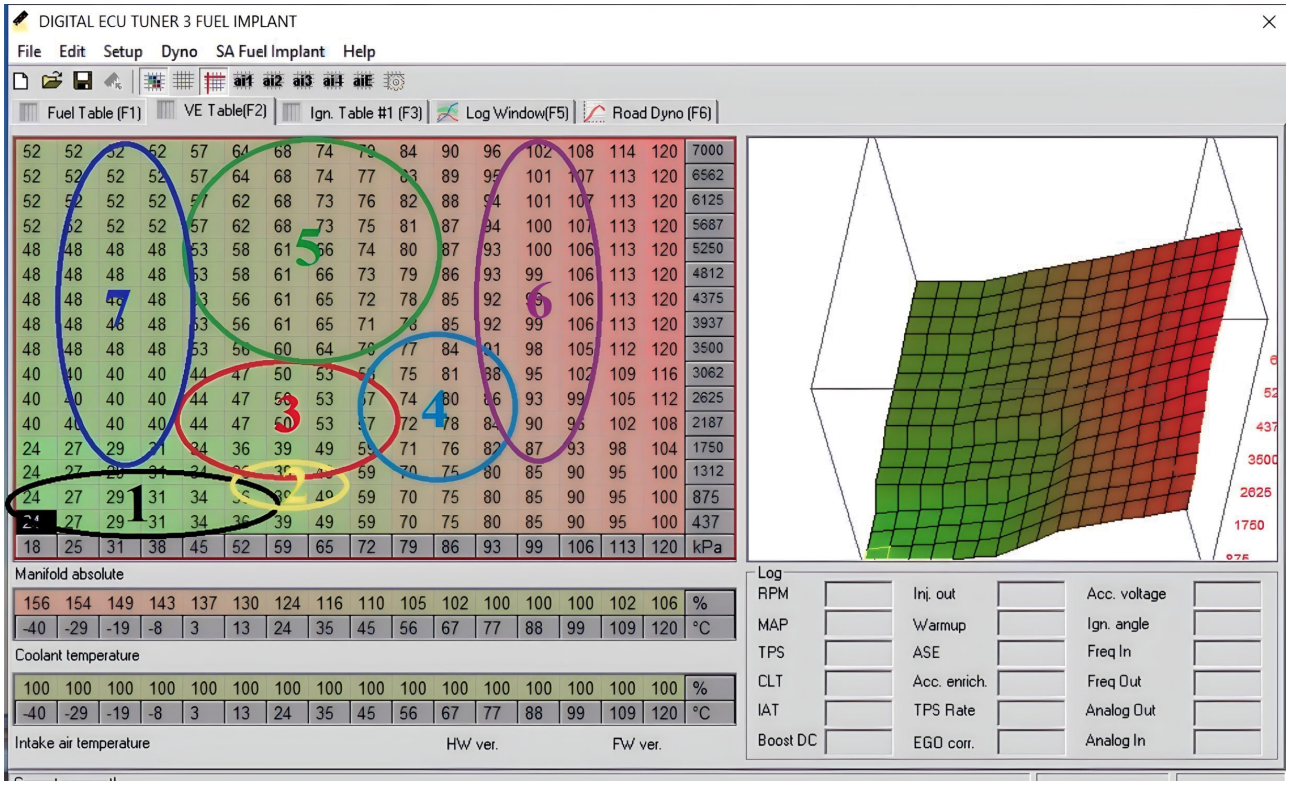

Figure 10. Sensors' and ECU's location.

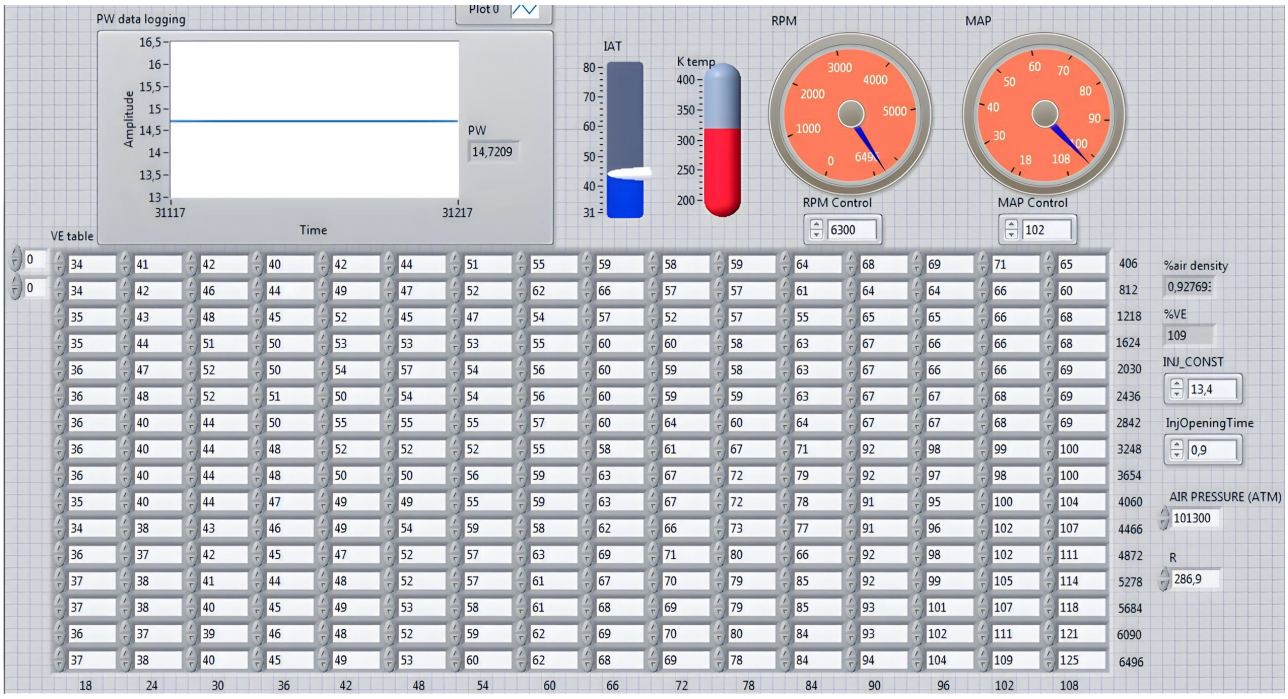

Figure 11. The front panel of the virtual control device is made in the LabVIEW program.

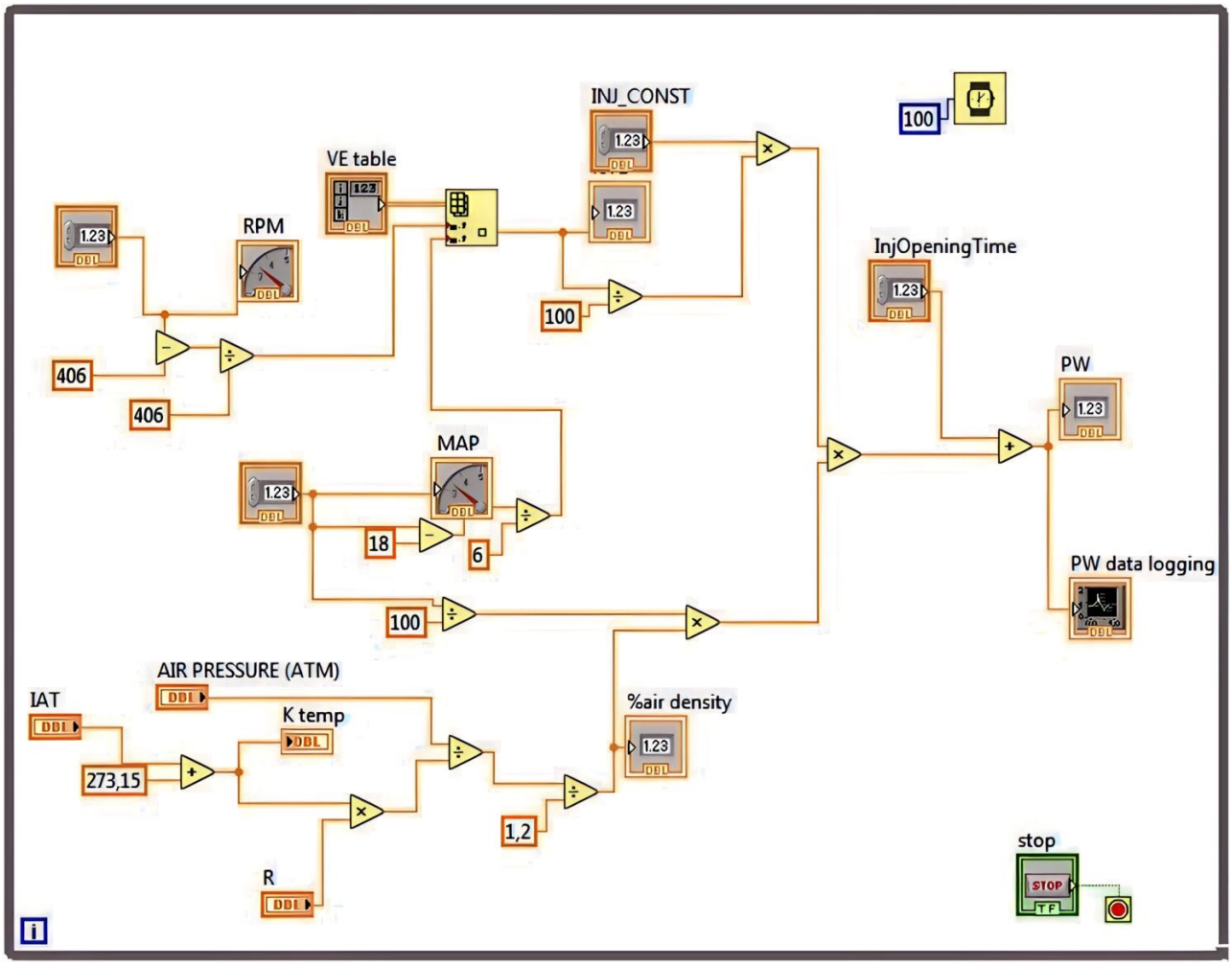

Figure 12. Block diagram of the fuel injection pulse width simulation.

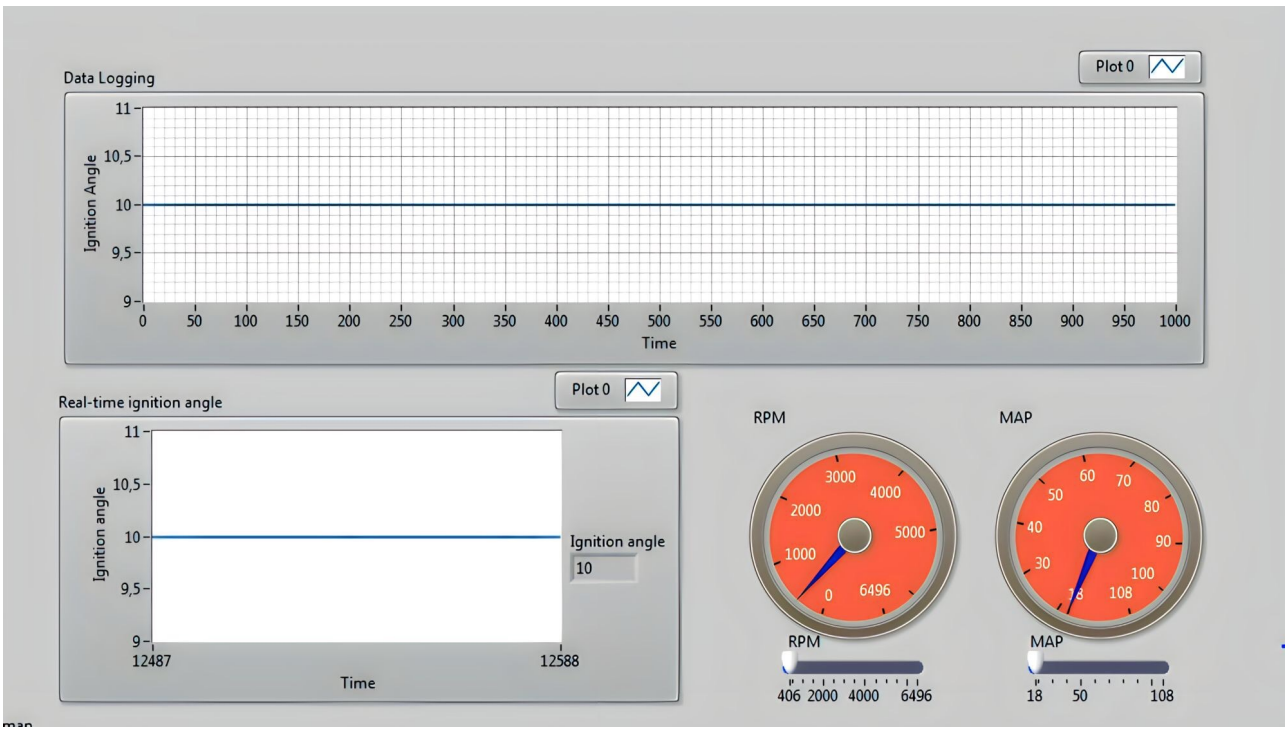

Figure 13. Front panel and ignition angle waveform of the virtual control device made in the LabVIEW program.

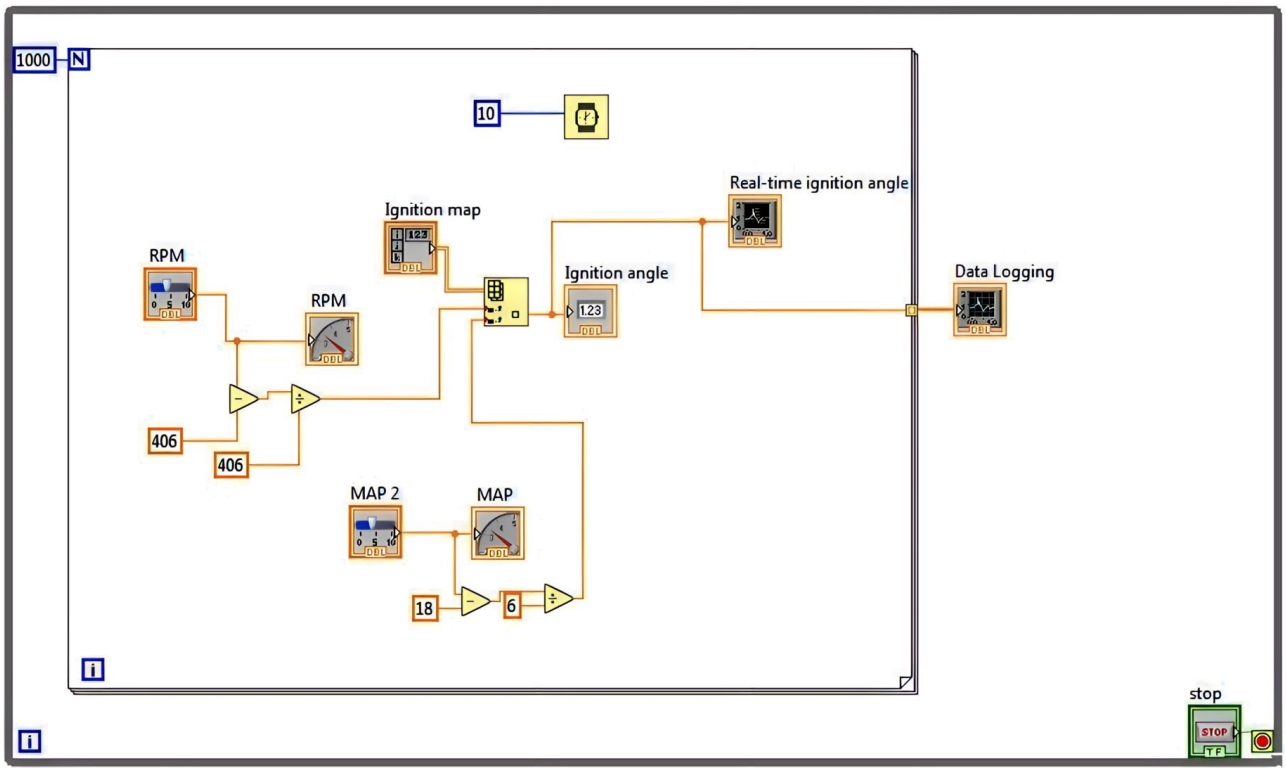

Figure 14. Block diagram of the ignition timing simulation.

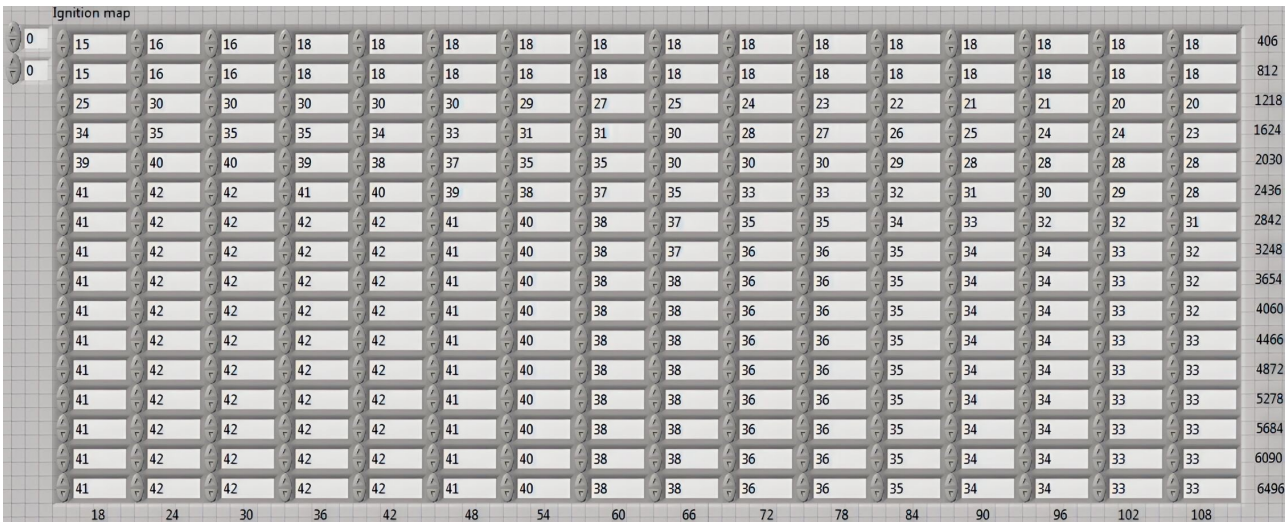

Figure 15. Ignition timing table.

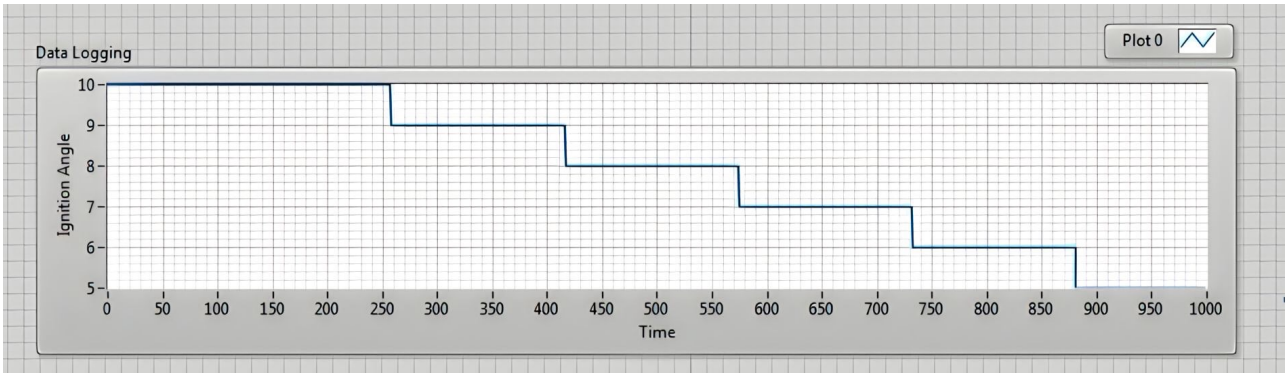

Figure 16. LabVIEW plot for Load Vs Ignition Angle.

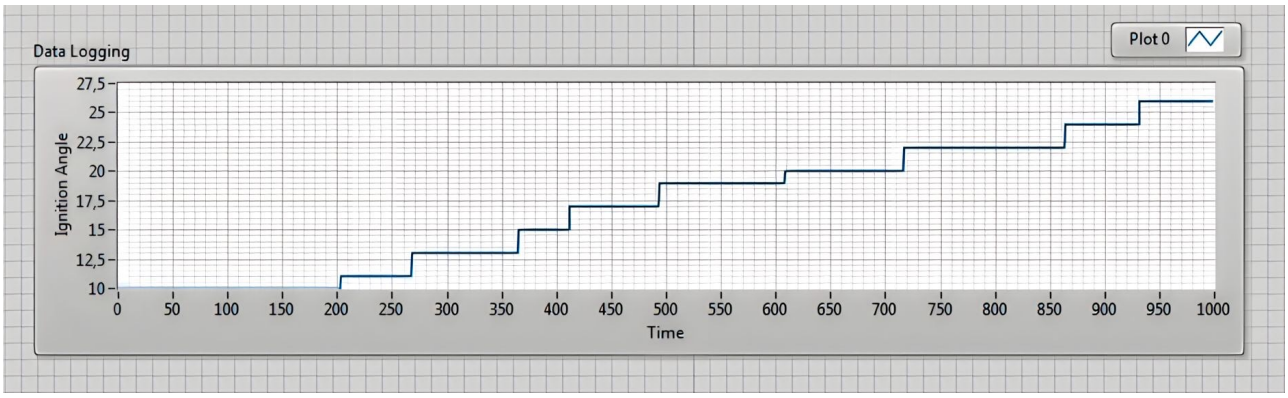

Figure 17. LabVIEW plot for Engine Speed Vs Ignition Angle.

Figure 18. Racebox measurement device.

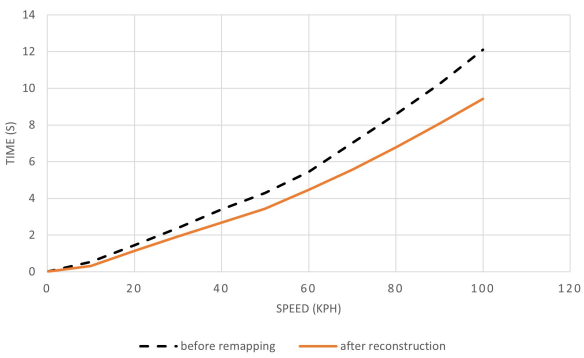

Figure 19. Acceleration time before and after remapping.

the vehicle via a computer and Racebox device. After the experiments, the measurement results were exported by the Racebox device in a CSV file format and imported into the chart in Figure 19 in order to demonstrate and compare these two results.

Figure 19 shows the difference between before and after the remapping was done. The The acceleration time 0–100 km·h^{-1} was decreased from 12.1 seconds to 9.42 seconds, equivalent to 23 %. It shows the power improvement when changing the fuel dose of the vehicle.

4.2. Experimental Data for Calculating Algorithm

Table 2 shows all engine parameters of the BMW E39, engine operation is used to calculate our algorithm. To carry out the calculations, the algorithm needs some parameters such as Injector constant (Inj-const), which is a constant dependent on the engine capacity, size of the injectors, and the Injection Divider parameter, and it represents the injector opening time which will yield a stoichiometric mixture with 100 % engine's volumetric efficiency, 100 KPa pressure, and 21°C temperature.

4.3. Fuel Injection Pulse Width and Air Fuel Ratio in the Idle Region of the Engine

There is a difference between the Piggyback ECU and the simulation algorithm, it can be seen around 800 RPM in Figure 20. The fuel injection pulse width was different between the experiment and the simulation within the idle region.

During the experiment, the fuel injection pulse width values were held at 3.3 ms, which means the engine does not stall and has a smooth control. Specifically, the pulse width experiment and the pulse width simulation has a difference of about 0.06–0.3 %. The difference is almost negligible due to the difference of the actual factor compared to the theory algorithm.

The Air-Fuel Ratio curve in Figure 21 shows AFR ranges in the Idle region. This curve is obtained from data logging of the on-road real-time experiment. The AFR cannot be kept at 14.7, due to certain factors, such as air density, barometric pressure, and enrichments. So, the AFR slightly fluctuates, but the mixture will be kept around 14.7. The AFR optimal value in this idle region, as stated by the manufacturer, is around 14.7, which is the stoichiometry mixture for gasoline, mentioned in Figure 1 in the Section 1. The AFR values were kept unchanged for idling, in order to achieve a better fuel economy and emissions.

N [RPM]	V_d [l]	MAP [kPa]	R_air	$InjOpening$ $time$ [ms]	$Inj\text{-}const$	Cps	MAT [°C]	$Pair$ [%]	N_v [%]	ΔT [ms]
850	2.5	51	286.9	0.9	13.4	2	60	0.882	48	3.796
1000	2.5	54	286.9	0.9	13.4	2	60	0.882	52	4.22
2000	2.5	48	286.9	0.9	13.4	2	56	0.893	57	4.17
3000	2.5	54	286.9	0.9	13.4	2	56	0.893	55	4.45
4000	2.5	101	286.9	0.9	13.4	2	45	0.924	100	13.41
5000	2.5	102	286.9	0.9	13.4	2	45	0.924	102	13.79
6300	2.5	102	286.9	0.9	13.4	2	44	0.927	109	14.72

TABLE 2. Experimental data were used to calculate our fuel pulse width algorithm.

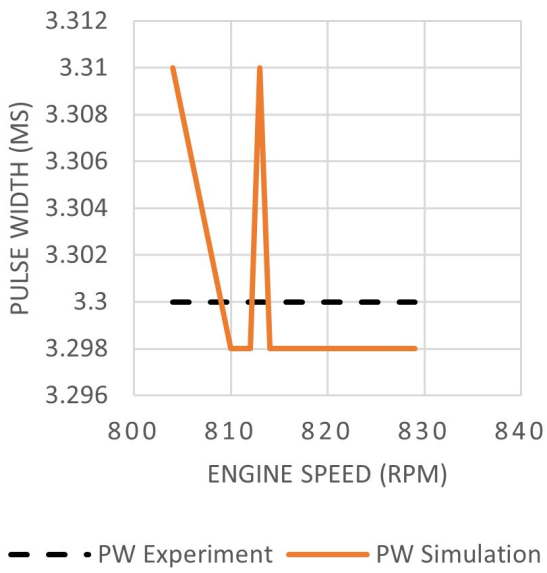

FIGURE 20. Pulse width comparison at Idle (around 800 RPM).

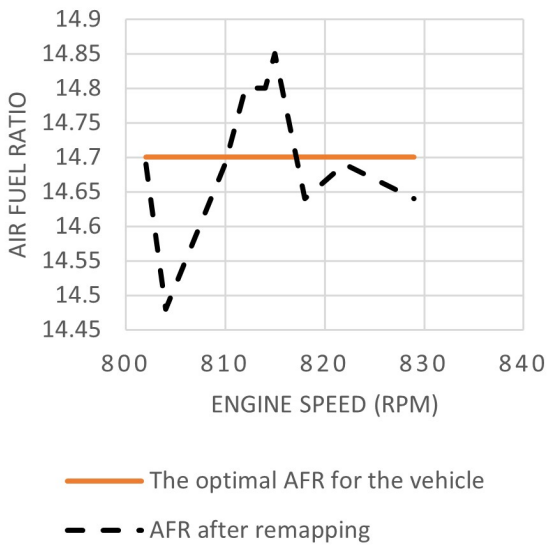

FIGURE 21. Air Fuel Ratio at Idle (around 800 RPM).

4.4. Fuel Injection Pulse Width and Air Fuel Ratio in the Cruise Region of the Engine

The engine will spend a majority of the time in the cruise region, especially when driving at a relatively steady speed on a smooth and flat road. A difference between the Piggyback ECU and the simulation algorithm can be seen between 1100–2300 RPM in Figure 22. The fuel injection pulse width were different between the experiment and the simulation in the cruise region. There is a difference of about 0.2–1.3 % between the simulation and the experimental values, the difference is almost negligible due to the difference of the actual factor compared to the theory algorithm.

The Air Fuel Ratio curve in Figure 23 shows AFR ranges in the cruise region. This curve is obtained from data logging of the on-road real-time experiment. The AFR optimal value in this region, as stated by the manufacturer, is around 14.7, which is the stoichiometry mixture for gasoline, mentioned in Figure 1 in Section 1. The AFR values were kept unchanged for idling, in order to achieve a better fuel economy and emissions.

4.5. Fuel Injection Pulse Width and Air Fuel Ratio in the WOT Region of the Engine

This WOT region is applied for a naturally aspirated engine. The manifold pressure in the WOT region will be equivalent to the atmospheric pressure. Achieving a maximum torque requires a fuel rich mixture. To effectively use the intake oxygen, the AFR for gasoline is usually set to 12. The additional fuel dose also makes the engine cooler when operating in high load, high RPM environments. There is a difference between Piggyback ECU and simulation algorithm observed between 3800–5800 RPM, as seen in Figure 24. The fuel injection pulse width was different between the experiment and the simulation in the WOT region. The difference between the pulse width for the experiment and the simulation was about 0–1.2 %, the difference is almost negligible due to the difference of the actual factor compared to the theory algorithm. Both fuel injection pulse width curves increase gradually from 3800 RPM to 5800 RPM with the same load at 102 kPa. That means the engine will produce more power in the WOT region.

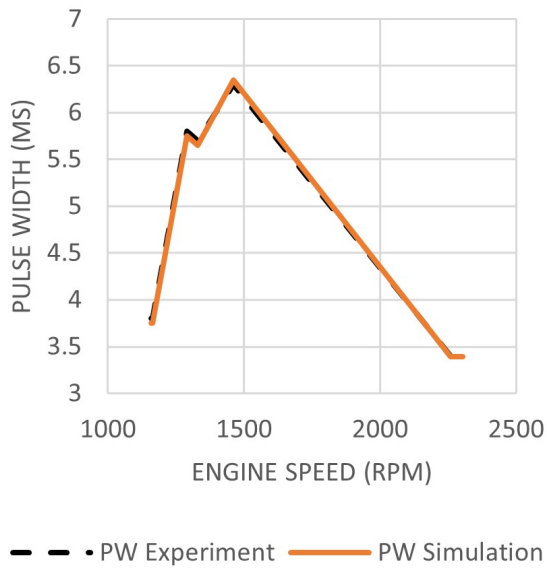

Figure 22. Pulse width comparison at Cruise (around 1100–2300 RPM).

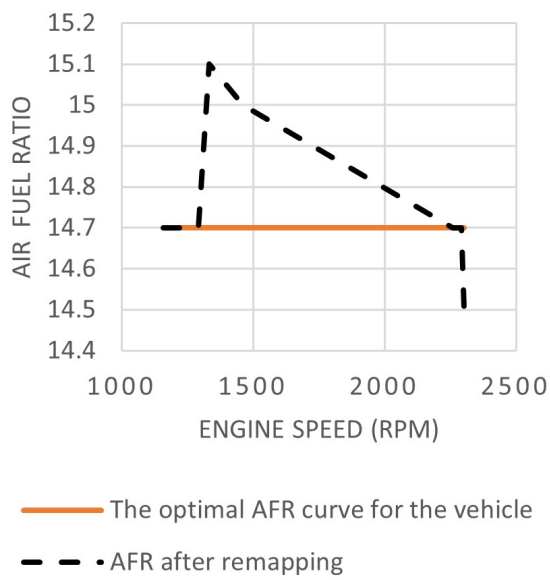

Figure 23. Air Fuel Ratio at Cruise (1100–2300 RPM).

The Air Fuel Ratio curve in Figure 25 shows AFR ranges in the WOT region. This curve is obtained from data logging of the on-road real-time experiment. The optimal AFR value in this region, as stated by the manufacturer, is 13.5. However, we set the values between 12.41 and 11.77, which are the values that yield the best performance for gasoline, as mentioned in Figure 1 in Section 1.

4.6. Ignition timing – Engine Speed Vs Ignition Angle

In this case, engine speeds are changed from low to high (shown in Figure 26). Ignition timing and engine speed are directly proportional. In the low RPM

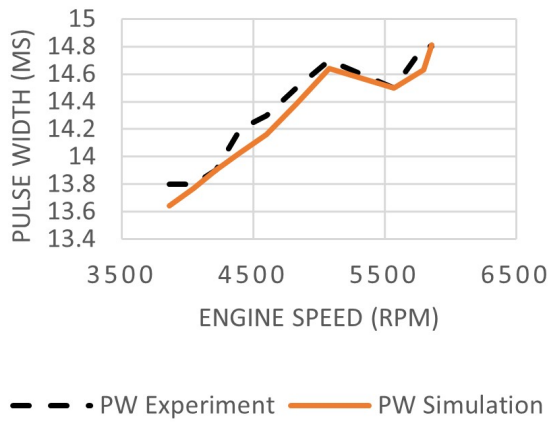

Figure 24. Pulse width comparison at WOT (around 3800–5800 RPM).

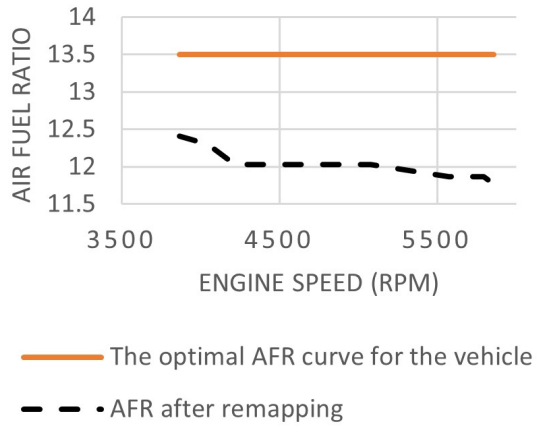

Figure 25. Air Fuel Ratio at WOT (around 3800–5800 RPM).

region, the ignition timing for half load and full load stays the same. At the next RPM region, the ignition timing for full load will be more advanced than for half load. Between 4450–6500 RPM, the spark angle remains constant.

4.7. Ignition timing – Engine Load Vs Ignition Angle

In this case, engine loads are changed from light to heavy and the engine speed is set to maximum (shown in Figure 27). Ignition timing and engine load are inversely proportional. At a low engine load, the ignition angle between the initial engine speed and full engine speed differs by 17 %, by 22 % at half load, and by 27 % at full load. It shows that the maximum load value directly affects the extent to which the ignition angle differs between the initial engine speed and the full engine speed.

5. Conclusion

The engine power is improved by changing the fuel injection pulse width at WOT. AFR values are de-

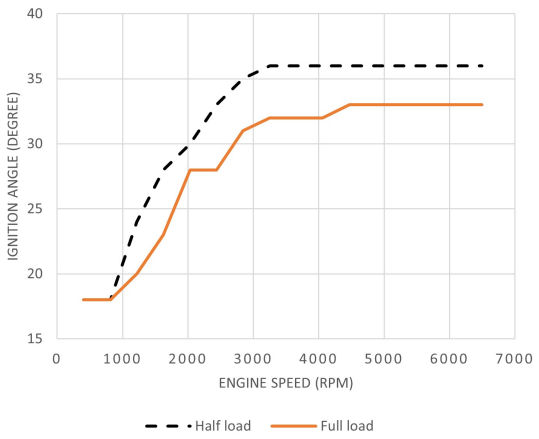

Figure 26. Engine Speed Vs Ignition Angle at half load and full load.

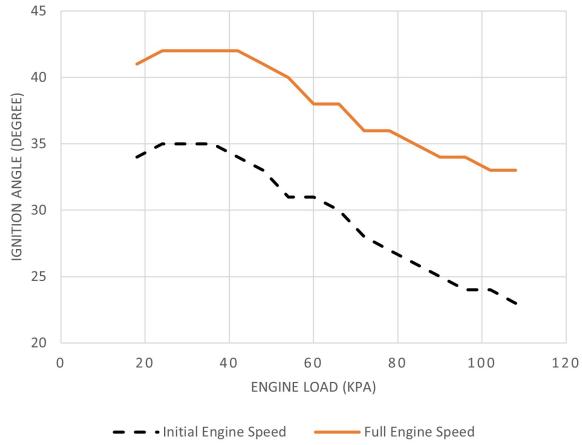

Figure 27. Engine Load Vs Ignition Angle at initial engine speed and full engine speed.

creased from 13.5 to 11.8 at WOT. In idle and cruise regions, AFR values were kept the same at 14.7 to optimise the fuel economy and emissions. These changes allow to reach higher speeds when one needs to, but also make the casual driving more comfortable. The acceleration times after the remapping decreased by approximately 23 %, as mentioned in the Analysis and Results section.

The advantage of this paper is that it can help people learn more about piggyback ECUs and how the SI engines work. The purpose of the LabVIEW simulation and the experiment is to better understand the operation algorithm of the electronic fuel injection system. The ignition timing simulation accurately represents the theoretical basis. But the codes were still not working flexibly and need to be further improved in the future, mainly in the aspect of determining the TDC from CKP sensor.

After carrying out the experiments on improving the engine performance with a piggyback ECU and analysing the results, we can conclude that the piggyback ECU, with all its advantages, is suitable for those who are starting their research on improving engine's performance, as well as for those who want to learn about basic algorithms in the electronic fuel injection systems.

In this paper, LabVIEW is used only for the simulation of fuel injector pulse width and ignition timing control, without the program directly controlling the vehicle. In order to use the LabVIEW program to control the vehicle, it needs to be improved to be able to read ECU parameters.

Acknowledgements

We would like to thank our instructor and editor Ph.D. Phu Thuong Luu Nguyen who helped us with all our questions and concerns regarding our paper. We would also like to thank PNA Auto Service Station, which sponsored us. Finally, we would like to thank our family and everyone who supported us during our project.

List of symbols

$\dot{m}_{intk}$ Engine intake port mass flow
$\dot{m}_{air}$ Engine intake air mass flow
V_d Engine displacement
Cps Crankshaft revolutions per power stroke
MAT Cycle average intake manifold pressure
R_{air} Ideal gas constant for air and burned gas mixture
f_{nv} Engine volumetric efficiency lookup table
AFR Air Fuel Ratio
ECU Electronic Control Unit
TDC Top Dead Centre
WOT Wide Open Throttle

References

[1] B. Mohamad, J. Karoly, A. Zelentsov. CFD modelling of formula student car intake system. *Facta Universitatis, Series: Mechanical Engineering* **18**(1):153–163, 2020. https://doi.org/10.22190/FUME190509032M

[2] B. Mohamad, A. Zelentsov. 1D and 3D modeling of modern automotive exhaust manifold. *Journal of the Serbian Society for Computational Mechanics* **13**(1):80–91, 2019. https://doi.org/10.24874/jsscm.2019.13.01.05

[3] P. Wong, X. Gao, K. Wong, et al. Initial-training-free online sequential extreme learning machine based adaptive engine air–fuel ratio control. *International Journal of Machine Learning and Cybernetics* **10**:2245–2256, 2019. https://doi.org/10.1007/s13042-018-0863-0

[4] M. Adamiec, M. Dziubiński. Alkaline fuel cell – aspect of efficiency. *Przeglad Elektrotechniczny* **85**(4):182–185, 2009. https://doi.org/10.1002/acm2.13208

[5] M. Dziubiński, A. Drozd, M. Adamiec, E. Siemionek. Electromagnetic interference in electrical systems of motor vehicles. *IOP Conference Series: Materials Science and Engineering* **148**:012036, 2016. https://doi.org/10.1088/1757-899X/148/1/012036

[6] M. Dziubiński, A. Drozd, M. Adamiec, E. Siemionek. Energy balance in motor vehicles. *IOP Conference Series: Materials Science and Engineering* **148**:012035, 2016. https://doi.org/10.1088/1757-899X/148/1/012035

[7] H. Nouraei, R. Benmrad, A. Sinclair. Development of a piezoelectric fuel injector. *Development of a Piezoelectric Fuel Injector* **65**(3):1162–1170, 2016. https://doi.org/10.1109/TVT.2015.2410136

[8] B. Ashok, S. Denis Ashok, C. Ramesh Kumar. A review on control system architecture of a si engine management system. *Annual Reviews in Control* **41**:94–118, 2016. https://doi.org/10.1016/j.arcontrol.2016.04.005

[9] F. Sprei, S. Karlsson, J. Holmberg. Better performance or lower fuel consumption: Technological development in the Swedish new car fleet 1975–2002. *Transportation Research Part D: Transport and Environment* **13**(2):75–85, 2008. https://doi.org/10.1016/j.trd.2007.11.003

[10] B. Mohamad, G. Szepesi, B. Bollo. Combustion optimization in spark ignition engines. In *MultiScience – XXXI. microCAD International Multidisciplinary Scientific Conference*. 2017. https://doi.org/10.26649/musci.2017.065

[11] U. Ibusuki, P. C. Kaminski. Product development process with focus on value engineering and target-costing: A case study in an automotive company. *International Journal of Production Economics* **105**(2):459–474, 2007. https://doi.org/10.1016/j.ijpe.2005.08.009

[12] K. Brundell-Freij, E. Ericsson. Influence of street characteristics, driver category and car performance on urban driving patterns. *Transportation Research Part D: Transport and Environment* **10**(3):213–229, 2005. https://doi.org/https://doi.org/10.1016/j.trd.2005.01.001

[13] L. Serrano, V. Carreira, R. Câmara, M. da Silva. On-road performance comparison of two identical cars consuming petrodiesel and biodiesel. *Fuel Processing Technology* **103**:125–133, 2012. https://doi.org/10.1016/j.fuproc.2011.12.012

[14] C. Tan, K. Tan, A. Tay. Computationally efficient behaviour based controller for real time car racing simulation. *Expert Systems with Applications* **37**(7):4850–4859, 2010. https://doi.org/10.1016/j.eswa.2009.12.030

[15] J. Kunanoppadol. The concept to measure the overall car performance. *The Journal of Science and Technology* pp. 4850–4859, 2013. https://doi.org/10.14456/jscitech.2013.102

[16] J. Heywood. *Internal Combustion Engine Fundamentals*. New York: McGraw-Hill, 1988.

[17] P. Saravana, C. Naiju. Electronic ignition of four stroke single cylinder engine. In *International Mobility Engineering Congress and Exposition*. 2009. https://doi.org/10.4271/2009-28-0024

[18] R. Bosch GmbH. Gasoline-engine management. Wiley, 2005.